



Furneaux, A. G., Piro, N. A., Hernández Sánchez, R., Gramigna, K. M., Fey, N., Robinson, M. J., Kassel, W. S., & Nataro, C. (2016). Spectroscopic, structural and computational analysis of  $[\text{Re}(\text{CO})_3(\text{dippM})\text{Br}]^{n+}$  (dippM = 1,1'-bis(diisopropylphosphino)metallocene, M = Fe, n = 0 or 1; M = Co, n = 1). *Dalton Transactions*, 45(11), 4819-4827.  
<https://doi.org/10.1039/c5dt04721h>

Peer reviewed version

Link to published version (if available):  
[10.1039/c5dt04721h](https://doi.org/10.1039/c5dt04721h)

[Link to publication record on the Bristol Research Portal](#)  
PDF-document

This is the author accepted manuscript (AAM). The final published version (version of record) is available online via RSC at <http://pubs.rsc.org/en/Content/ArticleLanding/2016/DT/C5DT04721H#!divAbstract>. Please refer to any applicable terms of use of the publisher.

## University of Bristol – Bristol Research Portal

### General rights

This document is made available in accordance with publisher policies. Please cite only the published version using the reference above. Full terms of use are available:  
<http://www.bristol.ac.uk/red/research-policy/pure/user-guides/brp-terms/>

Spectroscopic, structural and computational  
analysis of  $[\text{Re}(\text{CO})_3(\text{dippM})\text{Br}]^{n+}$  (dippM =  
1,1'-bis(diiso-propylphosphino)metallocene, M  
= Fe, n = 0 or 1; M = Co, n = 1)

Aliza G. Furneaux,<sup>a</sup> Nicholas A. Piro,<sup>b</sup> Raúl Hernández Sánchez,<sup>c</sup> Kathryn M.  
Gramigna,<sup>d</sup> Natalie Fey,<sup>e</sup> Michael J. Robinson,<sup>a</sup> W. Scott Kassel,<sup>b</sup> and Chip Nataro<sup>\*,a</sup>

<sup>a</sup>Department of Chemistry, Lafayette College, Easton, PA 18042, <sup>b</sup>Department of  
Chemistry, Villanova University, Villanova, PA 19085, <sup>c</sup>Department of Chemistry and  
Chemical Biology, Harvard University, Cambridge, MA 02138, <sup>d</sup>Department of  
Chemistry, Brandeis University, Waltham, MA 02454 and <sup>e</sup>School of Chemistry,  
University of Bristol, Cantock's Close, Bristol BS8 1TS, U.K.

\* Corresponding author. Tel.: +1 610 330 5216; fax: +1 610 330 5714.  
*E-mail address:* nataroc@lafayette.edu (C. Nataro).

## Abstract

---

While the redox active backbone of bis(phosphino)ferrocene ligands is often cited as an  
important feature of these ligands in catalytic studies, the structural parameters of  
oxidized bis(phosphino)ferrocene ligands have not been thoroughly studied. The

---

---

reaction of  $[\text{Re}(\text{CO})_3(\text{dippf})\text{Br}]$  ( $\text{dippf} = 1,1'$ -bis(diiso-propylphosphino)ferrocene) and  $[\text{NO}][\text{BF}_4]$  in methylene chloride yields the oxidized compound,  $[\text{Re}(\text{CO})_3(\text{dippf})\text{Br}][\text{BF}_4]$ . The oxidized species,  $[\text{Re}(\text{CO})_3(\text{dippf})\text{Br}][\text{BF}_4]$ , and the neutral species,  $[\text{Re}(\text{CO})_3(\text{dippf})\text{Br}]$ , are compared using X-ray crystallography, cyclic voltammetry, visible spectroscopy, IR spectroscopy and zero-field  $^{57}\text{Fe}$  Mössbauer spectroscopy. In addition, the magnetic moment of the paramagnetic  $[\text{Re}(\text{CO})_3(\text{dippf})\text{Br}][\text{BF}_4]$  was measured in the solid state using SQUID magnetometry and in solution by the Evans method. The electron transfer reaction of  $[\text{Re}(\text{CO})_3(\text{dippf})\text{Br}][\text{BF}_4]$  with acetylferrocene was also examined. For additional comparison, the cationic compound,  $[\text{Re}(\text{CO})_3(\text{dippc})\text{Br}][\text{PF}_6]$  ( $\text{dippc} = 1,1'$ -bis(diiso-propylphosphino)cobaltocenium), was prepared and characterized by cyclic voltammetry, X-ray crystallography, and NMR, IR and visible spectroscopies. Finally, DFT was employed to examine the oxidized dippf ligand and the oxidized rhenium complex,  $[\text{Re}(\text{CO})_3(\text{dippf})\text{Br}]^+$ .

---

## Introduction

The ligand 1,1'-bis(diphenylphosphino)ferrocene (dppf) is frequently employed in a variety of catalytic applications.<sup>1-3</sup> The catalytic efficiency, and therefore popularity of catalysts containing dppf and its various derivatives has been attributed to both steric and electronic factors. For 1,1'-bis(phosphino)ferrocene ligands, steric factors to consider include the steric bulk of the substituent groups on phosphorus,<sup>4</sup> the large bite angle imposed by the ferrocenyl backbone,<sup>5</sup> and the ability of the  $\text{C}_5$  rings to rotate which provides flexibility in coordination.<sup>6</sup> This last factor has been used to compare 1,1'-

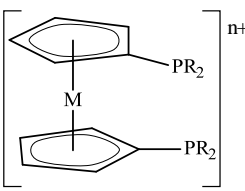
bis(phosphino)ferrocene ligands to a ball and socket joint<sup>6</sup> and has led to the moniker molecular ball bearings.<sup>7</sup> The two factors governing the electronic properties of these ligands are the substituents on the phosphorus atoms and the redox-active ferrocenyl backbone.<sup>1</sup> It is this last feature that is of particular relevance to this report.

The importance of the redox properties of ferrocene and its derivatives has been examined in a variety of different studies. A variety of compounds containing ferrocenyl moieties have been used as redox-switch catalysts, in which the catalytic activity of a compound with a ligand capable of existing in more than one valence state can be altered by varying the ligand valence. The activity of a ruthenium catalyst bound to a dendritic ferrocenyl cyclotriphosphazene is significantly decreased upon oxidation of the iron center.<sup>8</sup> Similarly, oxidation of the iron center in the catalyst [Y(phosphen)(O<sup>t</sup>Bu)] (phosphen = 1,1'-di(2-tert-butyl-6-diphenylphosphiniminophenoxy)ferrocene) completely halts the polymerization of  $\alpha$ -lactide.<sup>9</sup> For catalysts containing bis(phosphino)ferrocene ligands, the reduction of methyl viologen was found to be more efficient using [Cp\*(dppf)RuH][PF<sub>6</sub>] as compared to [Cp\*(dppf)RuH] as the catalyst.<sup>10</sup> The reactivities of [(Cym)(PP)RuCl][PF<sub>6</sub>] (Cym = 1-isopropyl-4-methylbenzene; PP = dppf or 1,1'-bis(diiso-propylphosphino)ferrocene (dippf)) have also been examined and these compounds are suggested to be useful redox-switch catalysts.<sup>11</sup>

Lacking from the studies employing bis(phosphino)ferrocene ligands are structures of these compounds in both the Fe(II) and Fe(III) valence states. For the free ligands, although the Fe(III) species is accessible, it is unlikely to be isolated and structurally characterized, as noted in the oxidation of dppf,<sup>12</sup> dippf<sup>13</sup> and 1,1'-bis(dicyclohexylphosphino)ferrocene (dcpf)<sup>14</sup> (Table 1), which were found to be

chemically irreversible due to reactions taking place at the phosphorus atoms following oxidation. The related compound, 1,1'-bis(ditert-butylphosphino)ferrocene (dtbpf), displays a reversible oxidation for the Fe(II/III) couple,<sup>15</sup> but neither valence state has been structurally characterized. The only structurally characterized compound in which the iron of the ferrocenyl backbone has been oxidized is [dppf]<sub>2</sub>[Sb<sub>4</sub>Cl<sub>16</sub>],<sup>16</sup> although it has been suggested that this compound actually be formulated as [dppf]<sub>4</sub>[Sb<sub>4</sub>Cl<sub>16</sub>].<sup>17</sup> The use of other chemical oxidants such as hydrogen peroxide,<sup>18-19</sup> sulfur<sup>18-19</sup> and bromine<sup>20</sup> again led to reactions at the phosphorus atoms as opposed to oxidation of the iron center.

**Table 1** 1,1'-bis(phosphino)metallocene ligands and abbreviations.

	<b>Ligand</b>	<b>R</b>	<b>M</b>	<b>M valence</b>	<b>n</b>
	dppf	Ph	Fe	II	0
	dippf	<sup>i</sup> Pr	Fe	II	0
	dippf <sup>+</sup>	<sup>i</sup> Pr	Fe	III	1
	dcpf	Cy	Fe	II	0
	dtbpf	<sup>t</sup> Bu	Fe	II	0
	dippc <sup>+</sup>	<sup>i</sup> Pr	Co	III	1

Coordination of the 1,1'-bis(phosphino)ferrocene ligands removes the potential complication of reactivity at the phosphorus atoms, thereby allowing the oxidation of the iron center to be more readily examined. Numerous studies have examined the oxidative electrochemistry of compounds containing dppf,<sup>1,12</sup> dippf,<sup>13</sup> dcpf<sup>14</sup> and dtbpf.<sup>15</sup> However, there have been relatively few reports of the isolation of these oxidation products which are typically obtained via chemical oxidation. The chemical oxidation of [Pd(dppf)Cl<sub>2</sub>] and [Pt(dppf)Cl<sub>2</sub>] by [NO][BF<sub>4</sub>] was found to give green, paramagnetic products.<sup>21</sup> A second study examined the Mössbauer spectrum of the Fe(III) complex [Pd(dppf)Cl<sub>2</sub>]<sup>+</sup> formed by the reaction of [Pd(dppf)Cl<sub>2</sub>] with [NO][BF<sub>4</sub>] after they were unable to isolate a product from the reaction of [Au<sub>2</sub>Cl<sub>2</sub>(dppf)] with [NO][BF<sub>4</sub>].<sup>22</sup> Using

spectroelectrochemistry and EPR spectroscopy, oxidation of [(Cym)Ru(dppf)Cl][PF<sub>6</sub>] (Cym = 1-isopropyl-4-methylbenzene) was determined to occur at the iron center, whereas oxidation of the closely related [Cp\*Ru(dppf)H] occurs at ruthenium.<sup>23</sup> The chemical and spectroelectrochemical oxidation of [Re(CO)<sub>3</sub>(dppf)Cl] has also been performed, and the Fe(III) product was characterized by IR and UV-Visible spectroscopies.<sup>24</sup> In addition, the oxidation of the closely related compounds [Re(CO)<sub>3</sub>(dppf)(OTf)] and [Re(CO)<sub>3</sub>(dppf)(MeCN)][OTf] has recently been examined spectroelectrochemically.<sup>25</sup> While all of these products have been characterized spectroscopically, to our knowledge there are no reported structures in which the coordinated 1,1'-bis(phosphino)ferrocene ligand has been oxidized. An analysis of the structural and electronic properties of a bis(phosphino)ferrocene ligand in both valence states would provide greater insight into the redox-switch catalytic activity of these ligands.

Previous studies in this laboratory examined the synthesis and spectroelectrochemistry of [Re(CO)<sub>3</sub>(dippf)Br].<sup>26</sup> Herein we report the isoelectronic [Re(CO)<sub>3</sub>(dippe)Br][PF<sub>6</sub>] (dippe = 1,1'-bis(diiso-propylphosphino)cobaltocenium) and the oxidized compound, [Re(CO)<sub>3</sub>(dippf)Br][PF<sub>6</sub>], containing an Fe(III) center. The paramagnetic [Re(CO)<sub>3</sub>(dippf)Br][PF<sub>6</sub>] was characterized by SQUID magnetometry and the two iron-containing species were examined by <sup>57</sup>Fe Mössbauer spectroscopy. X-ray crystal structures of all three compounds were obtained and the structural parameters were compared. In addition, DFT calculations were performed to examine the spin density in [Re(CO)<sub>3</sub>(dippf)Br][PF<sub>6</sub>].

## Results and discussion

The synthesis of  $[\text{Re}(\text{CO})_3(\text{dippc})\text{Br}][\text{PF}_6]$  was carried out using a method similar to the reported preparation of  $[\text{Re}(\text{CO})_3(\text{dippf})\text{Br}]$ .<sup>26</sup> The NMR spectral data for  $[\text{Re}(\text{CO})_3(\text{dippc})\text{Br}][\text{PF}_6]$  was found to be quite similar to that observed for  $[\text{Re}(\text{CO})_3(\text{dippf})\text{Br}]$  with the exception of the septet in the  $^{31}\text{P}\{^1\text{H}\}$  NMR spectrum that can be attributed to the  $[\text{PF}_6]^-$ . Similar to  $[\text{Re}(\text{CO})_3(\text{dippf})\text{Br}]^+$ , the  $\nu_{\text{CO}}$  stretches in the IR spectrum of  $[\text{Re}(\text{CO})_3(\text{dippc})\text{Br}][\text{PF}_6]$  are shifted 15-20  $\text{cm}^{-1}$  higher than the bands in  $[\text{Re}(\text{CO})_3(\text{dippf})\text{Br}]$  (Table 2). An analogous difference was noted in the IR spectra of the phenyl substituted complex,  $[\text{Re}(\text{CO})_3(\text{dppf})\text{Cl}]^{0/+}$ .<sup>24</sup> The  $\nu_{\text{CO}}$  stretches in these compounds are sensitive to the electron richness at the Re center. The bands shift to higher wavenumbers as the donor ability of the phosphine ligands decreases. The 15-20  $\text{cm}^{-1}$  is consistent upon oxidation of  $[\text{Re}(\text{CO})_3(\text{dppf})\text{Cl}]$  and  $[\text{Re}(\text{CO})_3(\text{dippf})\text{Br}]$ , suggesting that the decrease in donor ability of dppf and dippf upon oxidation is similar. In addition, the similar  $\nu_{\text{CO}}$  values for  $[\text{Re}(\text{CO})_3(\text{dippf})\text{Br}]^+$  and  $[\text{Re}(\text{CO})_3(\text{dippc})\text{Br}]^+$  signify that the donor ability of dippc<sup>+</sup> is comparable to that of dippf<sup>+</sup>.

**Table 2** Spectroscopic data for solutions of compounds in  $\text{CH}_2\text{Cl}_2$ .

	IR			Visible <sup>a</sup>	
	$\nu_{\text{CO}} (\text{cm}^{-1})$			$\lambda_{\text{max}} (\text{nm})$	$\epsilon (\text{M}^{-1} \text{cm}^{-1})$
dippf				445	110
$[\text{Re}(\text{CO})_3(\text{dippf})\text{Br}]^{\text{b}}$	2023 (vs)	1939 (m)	1888 (m)	429	150
$[\text{Re}(\text{CO})_3(\text{dippc})\text{Br}][\text{PF}_6]$	2038 (vs)	1957 (m)	1909 (m)	418	250
$[\text{Re}(\text{CO})_3(\text{dippf})\text{Br}][\text{BF}_4]$	2037 (vs)	1959 (m)	1908 (m)	614	100
$[\text{Re}(\text{CO})_3(\text{dppf})\text{Cl}]^{\text{c}}$	2035	1953	1900	436	159
$[\text{Re}(\text{CO})_3(\text{dppf})\text{Cl}]^{+\text{c}}$	2047	1972	1920	620	150

<sup>a</sup>For dippf and dippc<sup>+</sup> compounds, solutions were 0.2 mM. <sup>b</sup>Reference 26. <sup>c</sup>Reference 24.

The reaction of  $[\text{Re}(\text{CO})_3(\text{dippf})\text{Br}]$  with slightly more than one equivalent of  $[\text{NO}][\text{BF}_4]$  yields dark green  $[\text{Re}(\text{CO})_3(\text{dippf})\text{Br}][\text{BF}_4]$  in good yield. The change in the

UV-visible (Table 2) spectrum upon oxidation of the iron center to Fe(III) is similar to that which was observed for  $[\text{Re}(\text{CO})_3(\text{dppf})\text{Cl}]^{0/+}$ .<sup>24</sup> The  $\nu_{\text{CO}}$  stretches in the IR spectrum of  $[\text{Re}(\text{CO})_3(\text{dippf})\text{Br}]^+$  are in good agreement with the previously obtained spectroelectrochemical data.<sup>27</sup> No peak was observed in the  $^{31}\text{P}\{^1\text{H}\}$  NMR spectrum and significant broadening and paramagnetic shifts were observed in the  $^1\text{H}$  NMR spectrum. As suggested by the NMR data,  $[\text{Re}(\text{CO})_3(\text{dippf})\text{Br}]^+$  was determined to be paramagnetic. Using Evans method, the  $\mu_{\text{eff}}$  was determined to be 2.72(6) B.M. at 22.2°C. The temperature dependence of the magnetization was measured at 2-300 K and the  $\mu_{\text{eff}}$  remained constant (2.61 – 2.80 B.M.) from 50-300 K (Fig. 1). Curie-Weiss behavior was

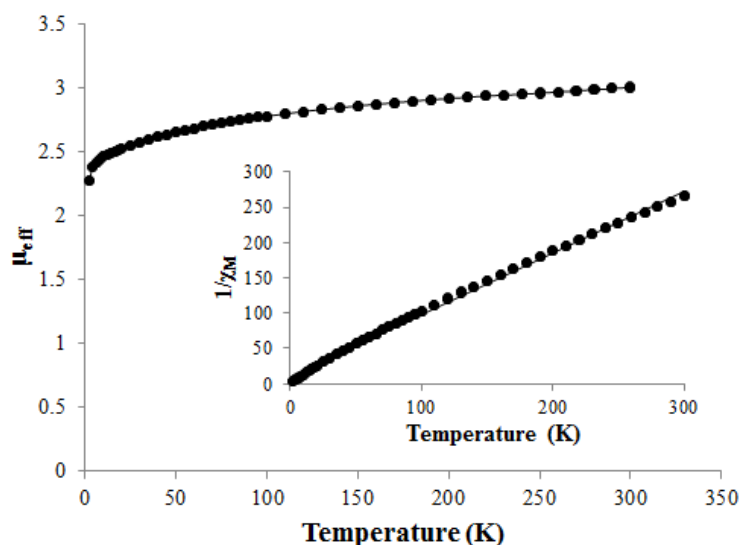


**Fig. 1** Temperature-dependent SQUID magnetization data for  $[\text{Re}(\text{CO})_3(\text{dippf})\text{Br}]^+$  plotted as magnetic moment ( $\mu_{\text{eff}}$ ) vs. T and  $1/\text{magnetic susceptibility}$  ( $\chi_M$ ) vs. T (inset).

noted over the temperature range of 50-300 K and the slope of the line gives a  $\mu_{\text{eff}}$  of 2.99 B.M. This value is significantly larger than that expected for a spin-only  $S = 1/2$  state, but is similar to the  $\mu_{\text{eff}}$  for ferrocenium,<sup>27</sup>  $[\text{CpFeCp}^*]^+$ ,<sup>28</sup> and decamethylferrocenium.<sup>29</sup> The larger than anticipated  $\mu_{\text{eff}}$  values in those systems have been attributed to the cations adopting  $^2\text{E}$  ground states that do not display significant low symmetry distortions<sup>27-29</sup> which is apparently also true for the coordinated  $\text{dippf}^+$  ligand in  $[\text{Re}(\text{CO})_3(\text{dippf})\text{Br}]^+$ .



To further examine the iron-containing compounds, the  $^{57}\text{Fe}$  Mössbauer spectra of dippf (Fig. 2a),  $[\text{Re}(\text{CO})_3(\text{dippf})\text{Br}]$  (Fig. 2b) and  $[\text{Re}(\text{CO})_3(\text{dippf})\text{Br}][\text{BF}_4]$  (Fig. 2c) were

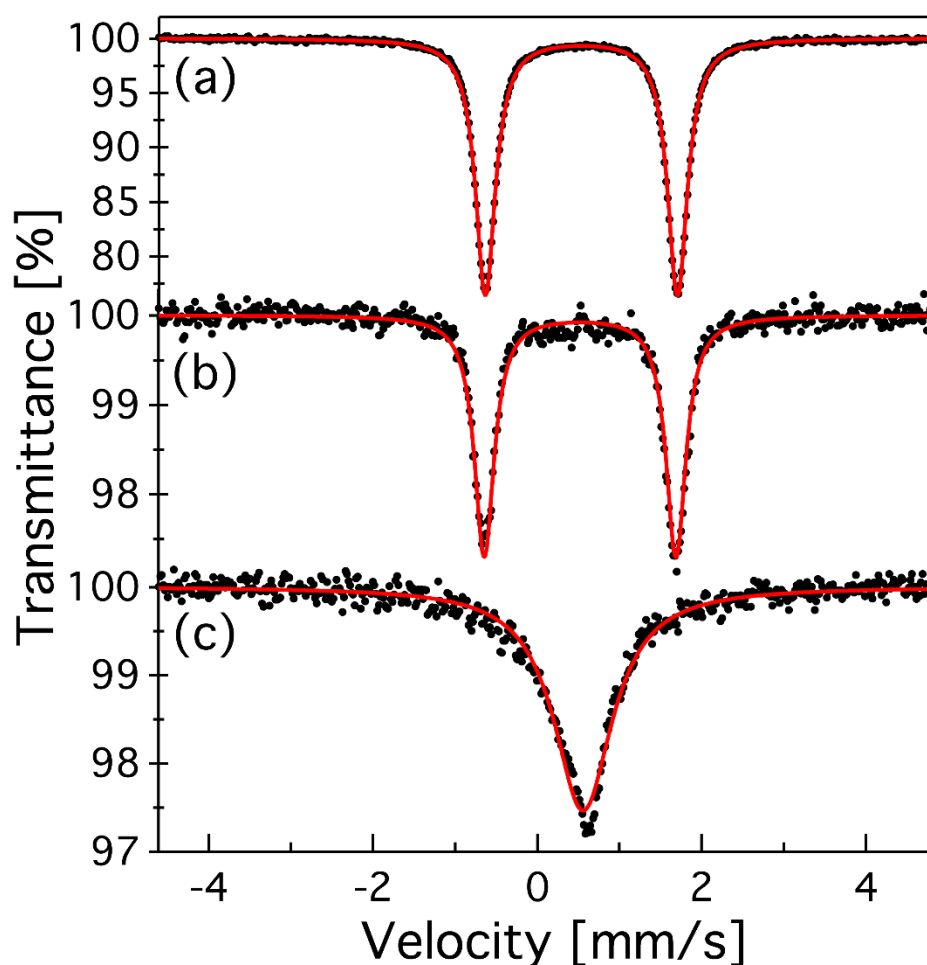


**Fig. 2** Zero-field  $^{57}\text{Fe}$  Mössbauer spectra of (a) dippf, (b)  $[\text{Re}(\text{CO})_3(\text{dippf})\text{Br}]$ , and (c)  $[\text{Re}(\text{CO})_3(\text{dippf})\text{Br}]^+$ .

obtained at 90 K. For dippf, the isomer shift ( $\delta$ ) was determined to be 0.54 mm/s, the quadrupole splitting ( $|\Delta E_Q|$ ) was 2.34 mm/s, and the full width at half maximum ( $\Gamma$ ) was 0.29 mm/s. These values are similar to those obtained for the related phenyl ligand, dppf, at comparable temperatures ( $\delta = 0.52$  mm/s and  $|\Delta E_Q| = 2.33$  mm/s at 77 K;<sup>21</sup>  $\delta = 0.53$  mm/s and  $|\Delta E_Q| = 2.30$  mm/s at 80 K<sup>30</sup>). Upon coordination there is very little change in both the  $\delta$  (0.53 mm/s),  $|\Delta E_Q|$  (2.33 mm/s) and  $\Gamma$  (0.29 mm/s) values for the iso-propyl substituted dippf ligand in  $[\text{Re}(\text{CO})_3(\text{dippf})\text{Br}]$ . Metal complexes containing dppf ligands

typically show a much greater difference in  $\delta$  and  $|\Delta E_Q|$  values as compared to free dppf; however, the values obtained for  $[\text{Re}(\text{CO})_3(\text{dippf})\text{Br}]$  do fall within the range expected for octahedral compounds containing a dppf ligand (Supporting Information Fig. S1).<sup>1,22,30</sup> It is well-known that the Mössbauer spectrum of ferrocenium ions display paramagnetic relaxation, which in turn gives rise to a single broad absorption line.<sup>31</sup> Oxidation of  $[\text{Re}(\text{CO})_3(\text{dippf})\text{Br}]$  gave a significant change in the  $^{57}\text{Fe}$  Mössbauer spectrum where a doublet is no longer discernible and instead a broad ( $\Gamma = 0.89$  mm/s) singlet, indicative of Fe(III) character, with  $\delta$  and  $|\Delta E_Q|$  values of 0.57 mm/s and 0 mm/s is observed. These differences are similar to the oxidation of  $[\text{Pd}(\text{dppf})\text{Cl}_2]$ , which had values of  $\delta = 0.51$  mm/s and  $|\Delta E_Q| = 2.24$  mm/s for the Fe(II) before oxidation and displays a broad singlet with  $\delta = 0.55$  mm/s and  $|\Delta E_Q| = 0$  mm/s for the Fe(III) after oxidation.<sup>22</sup>

DFT calculations support the presence of Fe(III) in  $[\text{Re}(\text{CO})_3(\text{dippf})\text{Br}]^+$ . The spin density for  $[\text{Re}(\text{CO})_3(\text{dippf})\text{Br}]^+$  is localized mainly on the  $\text{FeCp}_2$  unit ( $> 98\%$  in Mulliken and Natural Orbital spin densities at the UB3LYP level, with 77 and 78 % respectively located on the Fe atom) (Fig. 3). This is very similar to the calculated spin

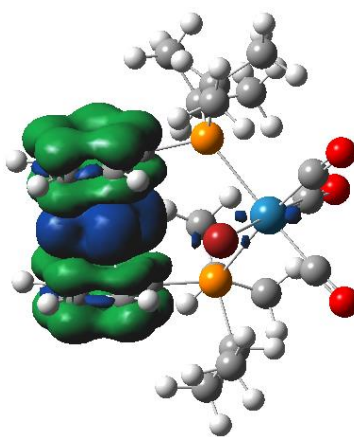


**Fig. 3** Plot of spin density for  $[\text{Re}(\text{CO})_3(\text{dippf})\text{Br}]^+$  calculated with UB3LYP, shown as an isosurface of 0.0004 au.

density for  $\text{dippf}^+$  which is almost completely localized on the  $\text{FeCp}_2$  unit as well (Supporting Information, Fig. S2).

The structures of  $[\text{Re}(\text{CO})_3(\text{dippf})\text{Br}]$  (Fig. 4),  $[\text{Re}(\text{CO})_3(\text{dippf})\text{Br}][\text{BF}_4]$  (Fig. 5) and  $[\text{Re}(\text{CO})_3(\text{dippe})\text{Br}][\text{PF}_6]$  (Fig. 6) were obtained at 100(2) K and selected bond lengths and angles are presented (Table 3). While similar, the structure of  $[\text{Re}(\text{CO})_3(\text{dippf})\text{Br}]$  reported herein deviates very slightly from the previously reported room temperature structure.<sup>32</sup> The largest differences are the Br-Re-P and  $\tau$  angles which are, respectively, approximately  $6^\circ$  and  $2^\circ$  smaller in the room temperature structure. Oxidation of the dippf ligand does not cause significant changes to the geometry around the rhenium atom. The bond lengths associated with the carbonyl ligands *trans* to the phosphorus atoms do not vary much,  $\Delta d(\text{Re}-\text{C}) = +0.006 \text{ \AA}$  and  $\Delta d(\text{C}-\text{O}) = +0.002 \text{ \AA}$ ,

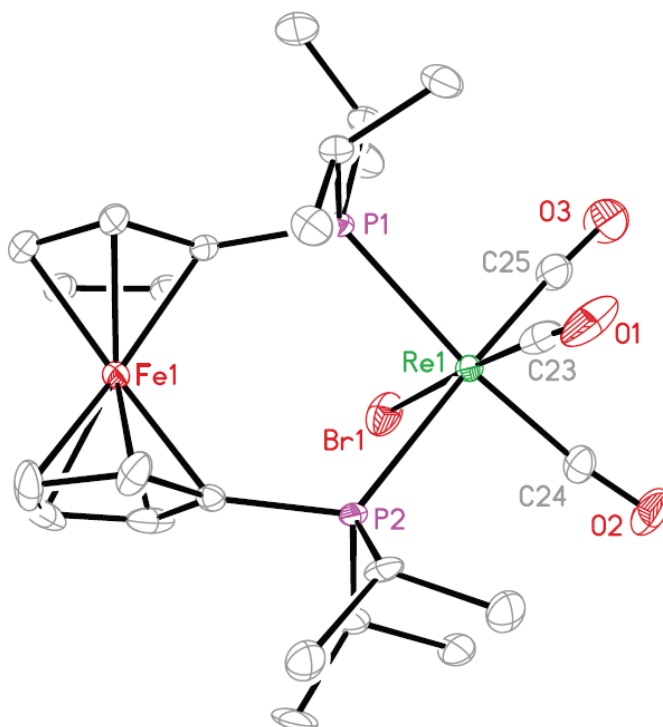


**Fig. 4** ORTEP drawing of  $[\text{Re}(\text{CO})_3(\text{dippf})\text{Br}]$ . Thermal ellipsoids are drawn at the 50% probability level and the H atoms were omitted for clarity.

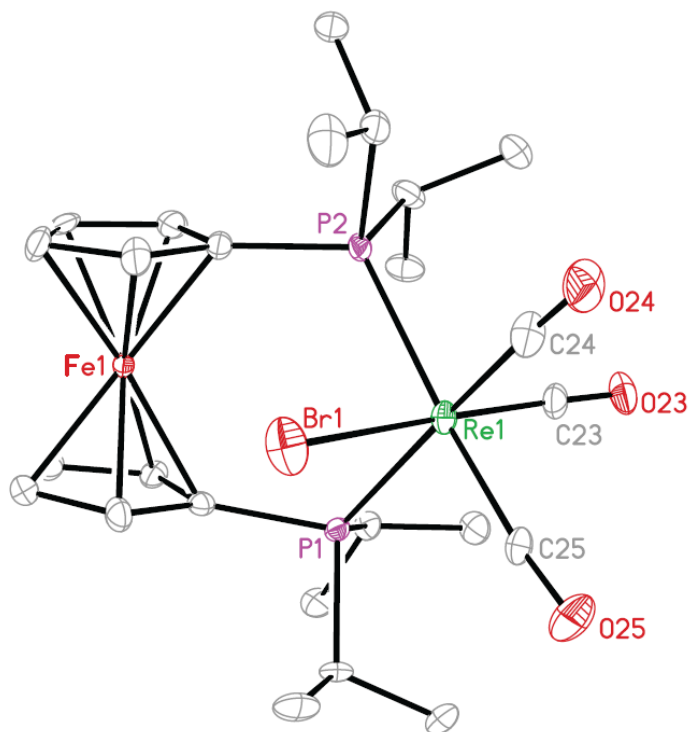


**Fig. 5** ORTEP drawing of  $[\text{Re}(\text{CO})_3(\text{dippf})\text{Br}][\text{BF}_4]$ . Thermal ellipsoids are drawn at the 50% probability level and the H atoms and  $[\text{BF}_4]^-$  were omitted for clarity. Only one of the crystallographically independent molecules is shown.

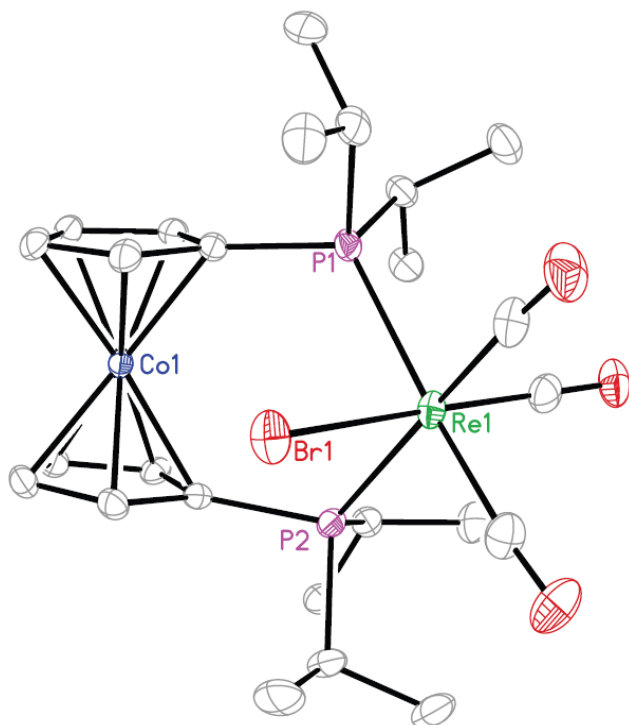


**Fig. 6** ORTEP drawing of  $[\text{Re}(\text{CO})_3(\text{dippe})\text{Br}][\text{PF}_6]$ . Thermal ellipsoids are drawn at the 50% probability level and the H atoms and  $[\text{PF}_6]^-$  were omitted for clarity.

upon oxidation of the dippf ligand. These changes are similar in magnitude to those observed for  $[(C_5H_4NH_2)Mn(CO)_3]^{0/+}$  and calculated for  $[CpRe(CO)_3]^{0/+}$ , in which oxidation occurs at the Group 7 metal center.<sup>33-34</sup> Changing the dippf ligand to the less electron donating dppe<sup>35</sup> or dippc<sup>+</sup> ligands results in similar differences; for the carbonyl ligands *trans* to the phosphorus atoms, the  $\Delta d(Re-C) = +0.002 \text{ \AA}$  and  $0.012 \text{ \AA}$  while  $\Delta d(C-O) = -0.004 \text{ \AA}$  and  $-0.005 \text{ \AA}$ , respectively. Minimal changes are also observed upon reduction of the cobalt center from Co(III) to Co(II) in  $[Re(CO)_4(dppe)]^{+2}$  (dppe = 1,1'-bis(diphenylphosphino)cobaltocenium), as  $\Delta d(Re-C) = +0.001 \text{ \AA}$  and  $\Delta d(C-O) = -0.010 \text{ \AA}$  for the carbonyl ligands *trans* to the phosphorus atoms.<sup>36</sup>

**Table 3** Select bond lengths (Å), bond angles (°) and structural parameters for  $[Re(CO)_3(dippf)Br]$ ,  $[Re(CO)_3(dippf)Br][BF_4]$  and  $[Re(CO)_3(dippc)Br][PF_6]$ .

	$[Re(CO)_3(dippf)Br]$	$[Re(CO)_3(dippf)Br][BF_4]$	$[Re(CO)_3(dippc)Br][PF_6]$
C-O (trans to P)	1.146 <sup>a</sup>	1.148 <sup>b</sup>	1.141 <sup>a</sup>
C-O (trans to Br)	1.098(4)	1.156 <sup>b</sup>	1.153(7)
Re-C (trans to P)	1.940 <sup>a</sup>	1.946 <sup>b</sup>	1.952 <sup>a</sup>
Re-C (trans to Br)	1.895(3)	1.900 <sup>b</sup>	1.902(5)
Re-P	2.522 <sup>a</sup>	2.524 <sup>b</sup>	2.5216 <sup>a</sup>
Re-Br	2.6213(8)	2.6066 <sup>b</sup>	2.6226(7)
M-X	1.6412 <sup>a</sup>	1.688 <sup>b</sup>	1.634
Re...M	4.5614(6)	4.461 <sup>b</sup>	4.4875(10)
Re-C-O (trans to P)	174.76 <sup>a</sup>	175.16 <sup>b</sup>	174.6 <sup>a</sup>
Re-C-O (trans to Br)	177.0(3)	176.2 <sup>b</sup>	176.0(5)
P-Re-P	96.31(2)	96.76 <sup>b</sup>	95.49(4)
Br-Re-P	92.82 <sup>a</sup>	88.18 <sup>b</sup>	88.21
X <sub>A</sub> -M-X <sub>B</sub>	176.47(8)	174.72 <sup>b</sup>	175.49(11)
$\tau^c$	12.13(18)	0.88 <sup>b</sup>	2.2(3)
$\theta^d$	3.55(11)	6.10 <sup>b</sup>	5.15(19)
$\delta_P^e$	-0.166 <sup>a</sup>	-0.089 <sup>b</sup>	-0.067 <sup>a</sup>
%V <sub>bur</sub>	47.0	46.8(2) <sup>f</sup>	46.4

<sup>a</sup>Average value. <sup>b</sup>Average value for two crystallographically independent molecules in the unit cell. <sup>c</sup>The torsion angle C<sub>A</sub>-X<sub>A</sub>-X<sub>B</sub>-C<sub>B</sub> where C is the carbon atom bonded to phosphorus and X is the centroid. <sup>d</sup>The dihedral angle between the two C<sub>5</sub> rings. <sup>e</sup>Deviation of the P atom from the C<sub>5</sub> plane; a positive value means the P is closer to the Fe. <sup>f</sup>Average deviation from the mean.

While oxidation of the dippf ligand appears to have little effect on the carbonyl ligands, there is an impact on the P-Re-P angle, which increases by 0.45° upon oxidation. This is likely due to the increased distance between the iron and the C<sub>5</sub> rings of the dippf

ligand upon oxidation. The distance between the iron atom and the centroid of the C<sub>5</sub> ring (Fe-X) in ferrocene increases by 0.044 Å upon oxidation.<sup>37</sup> A slightly larger increase is noted in this system. Likewise, the Co-X distance in cobaltocenium is 0.025 Å shorter than the corresponding Fe-X distance in ferrocene.<sup>38</sup> A slightly shorter metal to centroid distance is found in [Re(CO)<sub>3</sub>(dippc)Br]<sup>+</sup> compared to that of [Re(CO)<sub>3</sub>(dippf)Br], which would account for the 0.82° smaller P-Re-P angle observed in [Re(CO)<sub>3</sub>(dippc)Br]<sup>+</sup>. DFT-calculated structures generally agree with these observations, albeit with larger differences in M-centroid distances, a table of structural metrics can be found in the ESI, Table S1, alongside full computational details. Table S1 also shows the calculated structure for the cobaltocene complex [Re(CO)<sub>3</sub>(dippc)Br], which shows structural changes *cf.* the cobaltocenium form in line with expectations, *i.e.* a contraction of M-centroid distances.

The steric bulk of phosphine ligands can be quantified using the percent buried volume (%V<sub>bur</sub>).<sup>39</sup> Using the SambVca software<sup>40</sup> and previously recommended guidelines,<sup>39</sup> the %V<sub>bur</sub> values for five bidentate phosphines (P<sup>∧</sup>P) were calculated for [Re(CO)<sub>3</sub>(P<sup>∧</sup>P)Br] complexes from the crystal structures. In addition to the ligands investigated in this report (Table 1), the %V<sub>bur</sub> for dppf<sup>63</sup> and 1,1'-bis(dimethylphosphino)methane<sup>41</sup> (dmpm) were calculated to be 45.2(3) and 33.9 respectively. The %V<sub>bur</sub> for dippf, dippf<sup>+</sup> and dippc<sup>+</sup> are essentially indistinguishable. For dppf, dippf and dppm, the %V<sub>bur</sub> values for the [Re(CO)<sub>3</sub>(P<sup>∧</sup>P)Br] compounds are approximately 3% smaller than the values that were calculated for the corresponding [Mn(CO)<sub>3</sub>(P<sup>∧</sup>P)Br] compounds, likely due to the greater size of the Re atom as compared to Mn.<sup>26</sup>

The electrochemistry of these compounds was also examined. Previously, the oxidation of  $[\text{Re}(\text{CO})_3(\text{dippf})\text{Br}]$  was examined and found to give a reversible wave with  $E^\circ = 0.32 \text{ V vs. FcH}^{0/+}$ .<sup>26</sup> Under similar conditions, the reduction of  $[\text{Re}(\text{CO})_3(\text{dippf})\text{Br}]^+$  displays a reversible wave ( $i_{\text{rev}}/i_{\text{for}} = 0.96$ ,  $\Delta E_p = 80 \text{ mV}$ ) at  $0.32 \text{ V vs. FcH}^{0/+}$  as anticipated. The reduction of  $[\text{Re}(\text{CO})_3(\text{dippc})\text{Br}]^+$  (Fig. 7) also displays a single

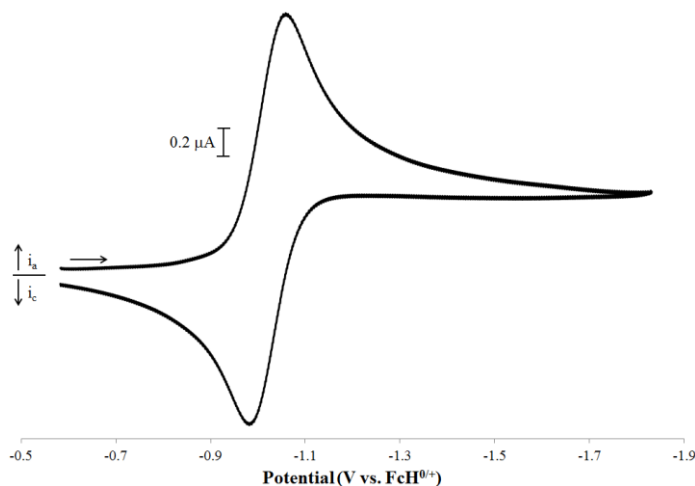


**Fig. 7** CV scan for the reduction of  $1.0 \text{ M } [\text{Re}(\text{CO})_3(\text{dippc})\text{Br}][\text{PF}_6]$  in  $\text{CH}_2\text{Cl}_2$  with  $[\text{NBu}_4][\text{PF}_6]$  as the supporting electrolyte at  $100 \text{ mV/s}$ .

reversible wave ( $i_{\text{rev}}/i_{\text{for}} = 0.96$ ,  $\Delta E_p = 77 \text{ mV}$ ) with  $E^\circ = -1.02 \text{ V vs. FcH}^{0/+}$ . The potential at which reduction of  $[\text{Re}(\text{CO})_3(\text{dippc})\text{Br}]^+$  occurs is  $0.11 \text{ V}$  more negative than the reported reduction potential for  $[\text{Re}(\text{CO})_3(\text{dppc})\text{Br}]^+$  in acetonitrile ( $-0.91 \text{ V vs. FcH}^{0/+}$ ).<sup>36</sup> This  $0.11 \text{ V}$  difference is precisely the same difference observed for the reduction potentials of the free ligands,  $\text{dppc}^+$  and  $\text{dippc}^+$  ( $-1.14$  and  $-1.25 \text{ V vs. FcH}^{0/+}$  respectively) in methylene chloride.<sup>42</sup> This suggests that the observed wave can be attributed to the reduction of  $\text{Co}(\text{III})$  to  $\text{Co}(\text{II})$ . A correlation between the redox potentials of compounds containing  $1,1'$ -bis(phosphino)ferrocene and  $1,1'$ -bis(phosphino)cobaltocenium ligands has been developed.<sup>43</sup> This correlation predicts a reduction potential of  $-0.98 \text{ V vs. FcH}^{0/+}$  for  $[\text{Re}(\text{CO})_3(\text{dippc})\text{Br}]^+$ , which is in good

agreement with the experimentally determined value. We have also explored calculating the one-electron redox potentials at the same level of theory as the reported geometry optimizations, following the previously described procedures.<sup>44</sup> These results, discussed more fully in the ESI, suggest that the cobaltocene couples are generally easier to oxidize than their ferrocene equivalents and that metallocene derivatization appears to make oxidation easier compared to the unsubstituted metallocene, while the rhenium complexation of these ligands raises the energy difference again.

The reaction of  $[\text{Re}(\text{CO})_3(\text{dippf})\text{Br}][\text{BF}_4]$  with acetylferrocene in  $\text{CH}_2\text{Cl}_2$  ( $E^\circ = 0.27 \text{ V vs. FcH}^{0/+}$ )<sup>45</sup> was performed in order to explore the electron transfer reactions of  $[\text{Re}(\text{CO})_3(\text{dippf})\text{Br}][\text{BF}_4]$ . An IR spectrum was obtained immediately after combining equimolar solutions of the two reagents. The  $\nu_{\text{CO}}$  region of the spectrum contained three peaks for the neutral  $[\text{Re}(\text{CO})_3(\text{dippf})\text{Br}]$  as well as a peak at  $1700 \text{ cm}^{-1}$  attributable to acetylferrocenium; a peak at  $1667 \text{ cm}^{-1}$  for acetylferrocene was noticeably absent (Supporting Information Fig. S3-S5).<sup>46</sup>

## Conclusions

Oxidation of  $[\text{Re}(\text{CO})_3(\text{dippf})\text{Br}]$  can be carried out using  $[\text{NO}][\text{BF}_4]$  as a chemical oxidant. Zero-field  $^{57}\text{Fe}$  Mössbauer spectroscopy was performed, and it was found that oxidation occurs at the iron center of the coordinated dippf ligand. The structures of  $[\text{Re}(\text{CO})_3(\text{dippf})\text{Br}]$  and  $[\text{Re}(\text{CO})_3(\text{dippf})\text{Br}]^+$  were determined, and there are minimal changes that occur in the structure upon oxidation. In particular, small increases in the Fe-C distances and the P-Re-P angle were noted. This suggests that bis(phosphino)ferrocene ligands can be best described as spring-loaded molecular ball



bearings, as not only do they have the ability to rotate about the C<sub>5</sub> rings, but the ligands also possess the ability to access different valences states, which allows for variability in the size of the ligand backbone. The reaction of [Re(CO)<sub>3</sub>(dippf)Br]<sup>+</sup> with acetylferrocene suggests a quick electron transfer between the two compounds. For additional comparison, the cobalt analog [Re(CO)<sub>3</sub>(dippc)Br]<sup>+</sup> was prepared and was found to be similar to [Re(CO)<sub>3</sub>(dippf)Br]<sup>+</sup> in terms of electron donor ability. Computational methods found that the redox potentials for the rhenium compounds as well as for the free phosphines and the metallocenes from which the compounds are derived follow the expected trends for ease of oxidation.

## Experimental

### General experimental methods

All preparative reactions were performed using standard Schlenk techniques under an atmosphere of argon. Methylene chloride (CH<sub>2</sub>Cl<sub>2</sub>), diethyl ether (Et<sub>2</sub>O), and hexanes were purified using a two-column Solv-tek system.<sup>47</sup> Chloroform was dried over molecular sieves and degassed prior to use. Reagents were used without additional purification unless otherwise noted. Ferrocene (FcH), dippf, diiso-propylchlorophosphine, decacarbonyl dirhenium [Re<sub>2</sub>(CO)<sub>10</sub>] and nitrosonium tetrafluoroborate ([NO][BF<sub>4</sub>]) were purchased from Strem. The FcH were sublimed prior to use. Tetrabutylammonium hexafluorophosphate ([NBu<sub>4</sub>][PF<sub>6</sub>]), ammonium hexafluorophosphate, dicyclopentadiene, *n*-BuLi (1.6 M in hexanes), hexachloroethane, cobalt(II) chloride hexahydrate (CoCl<sub>2</sub>•6H<sub>2</sub>O), acetylferrocene and bromine were purchased from Aldrich. The [NBu<sub>4</sub>][PF<sub>6</sub>] and CoCl<sub>2</sub>•6H<sub>2</sub>O were dried at 100 °C under vacuum. The compounds

[Re(CO)<sub>5</sub>Br],<sup>48</sup> [Re(CO)<sub>3</sub>Br(dippf)]<sup>26</sup> and [dippe][PF<sub>6</sub>]<sup>49</sup> were prepared according to the literature procedure. NMR spectra were obtained in CDCl<sub>3</sub> using a JEOL Eclipse 400 FT-NMR. The <sup>1</sup>H NMR spectra were referenced using internal TMS and the <sup>31</sup>P{<sup>1</sup>H} NMR spectra were referenced using external 85% H<sub>3</sub>PO<sub>4</sub>. IR spectra were recorded on a Matteson Satellite FT-IR. UV-Vis spectroscopy was performed on a Varian Cary Bio 300 UV-Vis spectrophotometer. Elemental analyses were performed by Quantitative Technologies, Inc.

### General synthetic chemical procedures

**[Re(CO)<sub>3</sub>(dippf)Br][BF<sub>4</sub>].** [Re(CO)<sub>3</sub>(dippf)Br] (0.1204 g, 0.1568 mmol) and [NO][BF<sub>4</sub>] (0.0214 g, 0.1833 mmol) were placed in a flask, degassed, and dissolved in 10 mL of CH<sub>2</sub>Cl<sub>2</sub>. The reaction mixture was stirred for 30 minutes during which time the color shifted from yellow to green-yellow. The volume of the solution was reduced to approximately 1 mL and then 10 mL of Et<sub>2</sub>O were added. The solution was placed in the freezer for 30 minutes during which time a green solid precipitated. The solution was filtered and the solid was recrystallized from CH<sub>2</sub>Cl<sub>2</sub> and Et<sub>2</sub>O. After filtering, the product was dried in vacuo and 0.1021 g (85% yield) of the product was obtained as a green solid. <sup>31</sup>P{<sup>1</sup>H} NMR: δ (ppm) no signal observed. <sup>1</sup>H NMR: δ (ppm) 16.18 (br, s), 12.33 (br, s), 5.61 (br, s), 1.30 (br, s). The μ<sub>eff</sub> was determined using Evans method by placing a sealed capillary tube containing CDCl<sub>3</sub> into a sample of [Re(CO)<sub>3</sub>(dippf)Br][BF<sub>4</sub>] with a known concentration in CDCl<sub>3</sub>. The reported value is the average of solutions with three different concentrations and the number in parenthesis is the average deviation from the mean. Anal. Calcd for C<sub>25</sub>H<sub>36</sub>BBrF<sub>4</sub>FeO<sub>3</sub>P<sub>2</sub>Re: C, 35.11; H, 4.24. Found: C, 34.89; H, 4.14.

**[Re(CO)<sub>3</sub>(dippe)Br][PF<sub>6</sub>].** [Re(CO)<sub>5</sub>Br] (0.0387 g, 0.0953 mmol) and [dippe][PF<sub>6</sub>] (0.0525 g, 0.0927 mmol) were placed in a flask and degassed. Chloroform (30 mL) was added and the bright orange solution was brought to reflux. The reaction refluxed over night during which time the solution turned a darker orange color. Upon cooling to room temperature, the solution was filtered via cannula. The solvent was then removed in vacuo and the resulting residue was recrystallized by dissolving the solid in 3 mL of CH<sub>2</sub>Cl<sub>2</sub> and then layering that solution with 10 mL of hexanes. The solution was then placed in a freezer overnight. The product precipitated from solution and the solution was filtered via cannula. The product was washed two times with 5 mL of Et<sub>2</sub>O and dried in vacuo. The product was collected as a bright orange solid (0.0494 g, 58% yield). <sup>31</sup>P{<sup>1</sup>H} NMR: δ (ppm) 8.53 (s), -143.7 (septet, <sup>1</sup>J<sub>P-F</sub> = 714 Hz). <sup>1</sup>H NMR: δ (ppm) 6.39 (br s, 2H, C<sub>5</sub>H<sub>4</sub>-), 6.02 (br s, 2H, C<sub>5</sub>H<sub>4</sub>-), 5.93 (br s, 2H, C<sub>5</sub>H<sub>4</sub>-), 5.87 (br s, 2H, C<sub>5</sub>H<sub>4</sub>-), 2.94 (m, 2H, -CH(CH<sub>3</sub>)<sub>2</sub>), 2.66 (m, 2H, -CH(CH<sub>3</sub>)<sub>2</sub>), 1.32 (m, 24H, -CH<sub>3</sub>). Anal. Calcd for C<sub>25</sub>H<sub>36</sub>BrCoF<sub>6</sub>O<sub>3</sub>P<sub>3</sub>Re: C, 32.76; H, 3.96. Found: C, 32.70; H, 3.92.

**Reaction of [Re(CO)<sub>3</sub>(dippf)Br][BF<sub>4</sub>] with acetylferrocene.** Acetylferrocene (0.0027 g, 0.012 mmol) was dissolved in CH<sub>2</sub>Cl<sub>2</sub> (0.5 mL). In a separate flask, [Re(CO)<sub>3</sub>(dippf)Br][BF<sub>4</sub>] (0.0103 g, 0.012 mmol) was dissolved in CH<sub>2</sub>Cl<sub>2</sub> (0.5 mL). The solutions were combined resulting in a dark green solution. An IR spectrum was obtained immediately after mixing the solutions.

### **X-ray diffraction studies**

Crystals of [Re(CO)<sub>3</sub>(dippf)Br], [Re(CO)<sub>3</sub>(dippf)Br][BF<sub>4</sub>] and [Re(CO)<sub>3</sub>(dippe)Br][PF<sub>6</sub>] were obtained by vapor diffusion of Et<sub>2</sub>O into a CH<sub>2</sub>Cl<sub>2</sub> solution of the respective compound. Single crystals were selected and mounted using

NVH immersion oil onto a glass fiber, a nylon fiber or a nylon loop and cooled to the data collection temperature of 100(2) K with a stream of dry nitrogen gas. Data were collected on a Bruker-AXS Kappa APEX II CCD diffractometer with 0.71073 Å Mo-K $\alpha$  radiation. Unit cell parameters were obtained from 60 data frames, 0.5°  $\phi$ , from three different sections of the Ewald sphere and complete data collection strategies were determined for each crystal using the APEX2 suite.<sup>50</sup> Each data set was refined using SAINT+<sup>51</sup> and treated with SADABS absorption corrections based on redundant multi-scan data.<sup>52</sup> The structures were solved by direct methods or intrinsic phasing and refined by least squares method on  $F^2$  using the SHELXL program package within APEX2.<sup>53</sup> All non-hydrogen atoms were refined with anisotropic displacement parameters and all hydrogen atoms were treated as idealized contributions, unless otherwise noted.

Data for [Re(CO)<sub>3</sub>(dippf)Br] were collected on a yellow block (0.30 x 0.20 x 0.15 mm<sup>3</sup>). The data set consisting of 123464 reflections (11759 unique,  $R_{int} = 0.0403$ ) was collected over  $\theta = 1.395$  to  $34.969^\circ$ . Systematic absences were consistent with the centrosymmetric, monoclinic space group  $C2/c$ . The asymmetric unit contains one molecule of [Re(CO)<sub>3</sub>(dippf)Br]. One of the P(<sup>i</sup>Pr)<sub>2</sub> moieties was disordered and modeled over two positions with the aid of similarity restraints on 1,2- and 1,3-distances as well as on anisotropic displacement parameters. The goodness of fit on  $F^2$  was 1.057 with  $R_1 = 2.83\%$  [ $I > 2\sigma(I)$ ],  $wR_2 = 6.27\%$  (all data) and with a largest difference peak and hole of 1.883 and  $-3.135 e/\text{Å}^3$ .

Data for [Re(CO)<sub>3</sub>(dippf)Br][BF<sub>4</sub>] were collected on a green plate (0.20 x 0.125 x 0.08 mm<sup>3</sup>). The data set consisting of 179573 reflections (24769 unique,  $R_{int} = 0.0936$ ) was collected over  $\theta = 2.254$  to  $34.338^\circ$ . Systematic absences were consistent with the

non-centrosymmetric, orthorhombic space group  $Pca2_1$ . The asymmetric unit contains two  $[\text{Re}(\text{CO})_3(\text{dippf})\text{Br}]^+$  cations and two  $\text{BF}_4^-$  anions. One  $[\text{BF}_4]^-$  anion was disordered over two positions and modeled with the aid of similarity restraints on 1,2- and 1,3-distances, as well as on anisotropic displacement parameters. The overlapping boron atoms were constrained to have identical anisotropic displacement parameters. Evaluation of the Flack parameter suggested refinement as a racemic twin and the twin ratio was freely refined to 72:28. The goodness of fit on  $F^2$  was 1.082 with  $R_1 = 4.56\%$  [ $I > 2\sigma(I)$ ],  $wR_2 = 9.43\%$  (all data) and with a largest difference peak and hole of 3.096 and  $-2.654 e/\text{\AA}^3$ .

Data for  $[\text{Re}(\text{CO})_3(\text{dippc})\text{Br}][\text{PF}_6]$  were collected on a yellow plate (0.30 x 0.15 x 0.02 mm<sup>3</sup>). The data set consisting of 10651 reflections (9823 unique,  $R_{int} = 0.0715$ ) was collected over  $\theta = 2.227$  to  $30.999^\circ$ . Systematic absences were consistent with the centrosymmetric, orthorhombic space group  $Pbca$ . The asymmetric unit contains one  $[\text{Re}(\text{CO})_3(\text{dippc})\text{Br}]^+$  cation and one  $[\text{PF}_6]^-$  anion. The goodness of fit on  $F^2$  was 1.209 with  $R_1 = 4.57\%$  [ $I > 2\sigma(I)$ ],  $wR_2 = 9.33\%$  (all data) and with a largest difference peak and hole of 2.137 and  $-1.685 e/\text{\AA}^3$ .

### Electrochemistry Procedure

A CH Instruments Model CHI260D potentiostat at room temperature ( $21 \pm 1^\circ\text{C}$ ) was employed for all cyclic voltammetry experiments. All experiments were performed under an atmosphere of argon. The concentration of the analytes was 1.0 mM in methylene chloride (10.0 mL) and the supporting electrolyte was 0.1 M  $[\text{NBu}_4][\text{PF}_6]$ . Experiments were performed with a glassy carbon working electrode (1.0 mm disk) that was polished with 1.0  $\mu\text{m}$  then 0.25  $\mu\text{m}$  diamond paste and rinsed with methylene

chloride prior to use. The experiments also employed a platinum wire counter electrode and a non-aqueous Ag/AgCl pseudo-reference electrode that was separated from the solution by a frit. Ferrocene was added at the end of the experiments and used as an internal reference. Data were background subtracted. Experiments were conducted at scan rates of 50 mV/s and 100 – 1000 mV/s in 100 mV/s increments. All data are reported at a scan rate of 100 mV/s.

### **Magnetic Susceptibility Measurements**

Magnetic measurements were recorded using a Quantum Design MPMS 3 SQUID magnetometer at 0.1 T. The magnetic susceptibility was adjusted for diamagnetic contributions using Pascal's constants.

### **Zero-field $^{57}\text{Fe}$ Mössbauer Spectroscopy**

Spectra were collected by restraining the samples in Paratone-N oil. The data were measured with a constant acceleration spectrometer (SEE Co., Minneapolis, MN). Isomer shifts are given relative to  $\alpha$ -Fe metal at 298 K. An in-house package written by Evan R. King in Igor Pro (Wavemetrics) was used for data analysis.

## **ASSOCIATED CONTENT**

### **Supporting Information**

Expected ranges for  $^{57}\text{Fe}$  Mössbauer spectra, computational details, summary of calculated structural data, calculated estimates for energy required in one-electron oxidations of metallocene complexes and xyz coordinates for all calculated structures are provided free of charge online at . Crystallographic data (CIF files) for the structural analysis have been deposited with the Cambridge Crystallographic Data Centre, CCDC No. 1438129 for

[Re(CO)<sub>3</sub>(dippf)Br][BF<sub>4</sub>], CCDC No. 1438130 for [Re(CO)<sub>3</sub>(dippf)Br], and CCDC No. 1438131 for [Re(CO)<sub>3</sub>(dippc)Br][PF<sub>6</sub>]. Copies of this information may be obtained free of charge from The Director, CCDC, 12 Union Road, Cambridge CB21EZ, UK, fax: +44 1223 336 033, e-mail: deposit@ccdc.cam.ac.uk or www: <http://www.ccdc.cam.ac.uk>.

## **AUTHOR INFORMATION**

### **Corresponding Author**

\*E-mail: nataroc@lafayette.edu

### **Notes**

The authors declare no competing financial interest.

## **ACKNOWLEDGEMENTS**

This work was supported in part by the National Science Foundation (CHE-1057795).

We thank the Kresge Foundation for the purchase of the JOEL NMR and the Academic Research Committee at Lafayette College for support through the EXCEL scholars program. R.H.S. acknowledges Consejo Nacional de Ciencia y Tecnología (CONACYT) and Fundación México for a doctoral fellowship. We thank the NSF MRI Grant DMR-1337567 for the SQUID grant to Boston College and K.M.G. thanks Professor Michael Graf (Boston College) for assistance with SQUID magnetometry. We thank Genevieve M. Asselin (Lafayette College Class of 2015) for her artistic interpretation of the spring-loaded molecular ball bearing dippf ligand.

## References

- 1) K.-S. Gan and T. S. A. Hor, 1,1'-Bis(diphenylphosphino)ferrocene - Coordination Chemistry, Organic Synthesis and Catalysis. In *Ferrocenes: Homogeneous Catalysis, Organic Synthesis, Materials Science*; A. Togni and T. Hayashi, Eds.; VCH: Weinheim, Germany, 1995; pp 3-104.
- 2) S. W. Chien and T. S. A. Hor, The Coordination and Homogeneous Catalytic Chemistry of 1,1'-Bis(diphenylphosphino)ferrocene and its Chalcogenide Derivatives. In *Ferrocenes: Ligands, Materials and Biomolecules*; P. Štěpnička, Ed.; John Wiley & Sons Ltd.: West Sussex, England, 2008; pp 33-116.
- 3) T. J. Colacot and S. Parisel, Synthesis, Coordination Chemistry and Catalytic Use of dppf Analogs. In *Ferrocenes: Ligands, Materials and Biomolecules*; P. Štěpnička, Ed.; John Wiley & Sons Ltd.: West Sussex, England, 2008; pp 117-140.
- 4) M. Kawatsura and J.F. Hartwig, *J. Am. Chem. Soc.*, 1991, **121**, 1473.
- 5) R. J. van Haaren, K. Goubitz, J. Fraanje, G. P. F. van Strijdonck, H. Oevering, B. Coussens, J. N. H. Reek, P. C. J. Kamer and P. W. N. M. van Leeuwen, *Inorg. Chem.*, 2001, **40**, 3363.
- 6) D. J. Young, S. W. Chien and T. S. A. Hor, *Dalton Trans.*, 2012, **41**, 12655.
- 7) P. Štěpnička, *Patai's Chemistry of Functional Groups - A Concise Introduction and Update*, 2012, 1.
- 8) P. Neumann, H. Dib, A.-M. Caminade and E. Hey-Hawkins, *Angew. Chem.*, 2015, **54**, 311
- 9) E. M. Broderick, N. Guo, C. S. Vogel, C. Xu, J. Sutter, J. T. Miller, K. Meyer, P. Mehrkhodavandi and P. L. Diaconescu, *J. Am. Chem. Soc.*, 2011, **133**, 9278.
- 10) R. T. Hembre, J. S. McQueen and V. W. Day, *J. Am. Chem. Soc.*, 1996, **118**, 798.
- 11) T. Sixt, M. Sieger, M. J. Krafft, D. Bubrin, J. Fiedler and W. Kaim, *Organometallics*, 2010, **29**, 5511.
- 12) C. Nataro, A. N. Campbell, M. A. Ferguson, C. D. Incarvito and A. L. Rheingold, *J. Organomet. Chem.*, 2003, **673**, 47.
- 13) J. H. L. Ong, C. Nataro, J. A. Golen and A. L. Rheingold, *Organometallics*, 2003, **22**, 5027.
- 14) L. E. Hagopian, A. N. Campbell, J. A. Golen, A. L. Rheingold and C. Nataro, *J. Organomet. Chem.*, 2006, **691**, 4890.
- 15) F. N. Blanco, L. E. Hagopian, W. R. McNamara, J. A. Golen, A. L. Rheingold and C. Nataro, *Organometallics*, 2006, **25**, 4292.
- 16) I. A. Razak, A. Usman, H.-K. Fun, B. M. Yamin and N. A. Kasim, *Acta Crystallogr., Sect. C: Cryst. Struct. Commun.*, 2002, **58**, m162.
- 17) S. Chatterjee, J. A. Krause, W. B. Connick, C. Genre, A. Rodrigue-Witchel and C. Reber, *Inorg. Chem.*, 2010, **49**, 2808.
- 18) J. J. Bishop, A. Davidson, M. L. Katcher, D. W. Lichtenberger, R. E. Merrill and J. C. Smart, *J. Organomet. Chem.*, 1971, **27**, 241.
- 19) B. D. Swartz and C. Nataro, *Organometallics*, 2005, **24**, 2447.
- 20) T. S. A. Hor, H. S. O. Chan, K.-L. Tan, L.-T. Phang, Y. K. Yan, L.-K. Liu and Y.-S. Wen, *Polyhedron*, 1991, **10**, 2347.



- 21) B. Corain, B. Longato, C. Favero, D. Ajó, G. Pilloni, U. Russo and F. R. Kreissl, *Inorg. Chim. Acta*, 1989, **157**, 259.
- 22) A. Houlton, R. M. G. Roberts, J. Silver and R. V. Parish, *J. Organomet. Chem.*, 1991, **418**, 269.
- 23) T. Sixt, J. Fielder and W. Kaim, *Inorg. Chem. Commun.*, 2000, **3**, 80.
- 24) T. M. Miller, K. J. Ahmed and M. S. Wrighton, *Inorg. Chem.*, 1989, **28**, 2347.
- 25) S. Roy, T. Blane, A. Lilio and C. P. Kubiak, *Inorg. Chim. Acta*, 2011, **374**, 134.
- 26) J. Berstler, A. Lopez, D. Ménard, W. G. Dougherty, W. S. Kassel, A. Hansen, A. Daryaei, P. Ashitey, M. J. Shaw, N. Fey and C. Nataro *J. Organomet. Chem.*, 2012, **712**, 37.
- 27) D. N. Hendrickson, Y. S. Sohn and H. B. Gray, *Inorg. Chem.*, 1971, **10**, 1559.
- 28) J. S. Miller, D. T. Glatzhofer, C. Vazquez, R. S. McLean, J. C. Calabrese, W. J. Marshall and J. W. Radbiger, *Inorg. Chem.*, 2001, **40**, 2058.
- 29) J. S. Miller, J. C. Calabrese, H. Rommelmann, S. R. Chittipeddi, J. H. Zhang, W. M. Reiff and A. J. Epstein, *J. Am. Chem. Soc.*, 1987, **109**, 769.
- 30) A. Houlton, S. K. Ibrahim, J. D. Dilworth and J. Silver, *J. Chem. Soc. Dalton Trans.*, 1990, 2421.
- 31) M. Abraham, H.-H. Klauß, W. Wagener, F.J. Litterst, A. Hofmann and M. Herberhold, *Hyperfine Interact.*, **1999**, 120, 253.
- 32) I. R. Butler, M. E. Light and M. B. Hursthouse, (1998) *University of Southampton, Crystal Structure Report Archive*. (doi:10.5258/ecrystals/747).
- 33) D. R. Laws, D. Chong, K. Nash, A. L. Rheingold and W. E. Geiger, *J. Am. Chem. Soc.*, 2008, **130**, 9859.
- 34) D. Chong, D. R. Laws, A. Nafady, P. J. Costa, A. L. Rheingold, M. J. Calhorda and W. E. Geiger, *J. Am. Chem. Soc.*, 2008, **130**, 2692.
- 35) M. A. Beckett, D. S. Brassington, S. J. Coles, T. Gelbrich, M. E. Light and M. B. Hursthouse, *J. Organomet. Chem.*, 2003, **688**, 174.
- 36) I. M. Lorković, M. S. Wrighton and W. M. Davis, *J. Am. Chem. Soc.*, 1994, **116**, 6220.
- 37) (a) B. W. Sullivan and B. M. Foxman, *Organometallics*, 1983, **2**, 187. (b) R. Martinez and A. Tiripicchio, *Acta Crystallogr.*, 1990, **C46**, 202.
- 38) D. Braga, L. Scaccianoce, F. Grepioni and S. M. Draper, *Organometallics*, 1996, **15**, 4675.
- 39) H. Clavier and S. P. Nolan, *Chem. Commun.*, 2010, **46**, 841.
- 40) (a) A. Poater, B. Cosenza, A. Correa, S. Giudice, F. Ragone, V. Scarano and L. Cavallo, *Eur. J. Inorg. Chem.*, 2009, 1759. (b) <http://www.molnac.unisa.it/OMtools/sambvca.php>.
- 41) J. T. Mague, *Acta Cryst. Sect. C: Crystallogr. Struct. Commun.*, 1994, **50**, 1391.
- 42) K. D. Reichl, C. L. Mandell, O. D. Henn, W. G. Dougherty, W. S. Kassel and C. Nataro, *J. Organomet. Chem.*, **2011**, 696, 3882.
- 43) J. K. Pagano, E. C. Sylvester, E. P. Warnick, W. G. Dougherty, N. A. Piro, W. S. Kassel and C. Nataro, *J. Organomet. Chem.*, 2014, **750**, 107.
- 44) (a) L. E. Roy, E. Jakubikova, M. G. Guthrie and E. R. Batista, *J. Phys. Chem. A*, 2009, **113**, 6745. (b) S. J. Konezny, M. D. Doherty, O. R. Luca, R. H. Crabtree, G. L. Soloveichik and V. S. Batista, *J. Phys. Chem. C*, 2012, **116**, 6349.
- 45) N. G. Connelly and W. E. Geiger, *Chem. Rev.*, 1996, **96**, 877.

- 46) M. J. Shaw and W. E. Geiger, *Organometallics*, 1996, **15**, 13.
- 47) A. B. Pangborn, M. A. Giardello, R. H. Grubbs, R. K. Rosen and F. J. Timmers, *Organometallics*, 1996, **15**, 1518.
- 48) R. J. Angelici, *Inorg. Synth.*, 1990, **28**, 162.
- 49) G.-A. Yu, Y. Ren, J.-T. Guan, Y. Lin and S. H. Liu, *J. Organomet. Chem.*, 2007, **692**, 3914.
- 50) APEX II, version 2012.10-0; Bruker AXS, Madison, WI, 2012.
- 51) SAINT+, version 8.26A: Data Reduction and Correction Program; Bruker AXS, Madison, WI, 2011.
- 52) SADABS, version 2012/1: An Empirical Absorption Correction Program; Bruker AXS, Madison, WI, 2012.
- 53) G. M. Sheldrick, SHELXTL, version 2012.10-2: Structure Determination Software Suite; Bruker AXS, Madison, WI, 2012.

Spectroscopic, structural and computational  
analysis of  $[\text{Re}(\text{CO})_3(\text{dippM})\text{Br}]^{n+}$  (dippM =  
1,1'-bis(diiso-propylphosphino)metallocene, M  
= Fe, n = 0 or 1; M = Co, n = 1)

Aliza G. Furneaux, Nicholas A. Piro, Raúl Hernández Sánchez, Kathryn M. Gramigna,  
Natalie Fey, Michael J. Robinson, W. Scott Kassel, and Chip Nataro\*



For table of contents use only

Spectroscopic, structural and computational  
analysis of  $[\text{Re}(\text{CO})_3(\text{dippM})\text{Br}]^{n+}$  (dippM =  
1,1'-bis(diiso-propylphosphino)metallocene, M  
= Fe, n = 0 or 1; M = Co, n = 1)

Aliza G. Furneaux, Nicholas A. Piro, Raúl Hernández Sánchez, Kathryn M. Gramigna,  
Natalie Fey, Michael J. Robinson, W. Scott Kassel, and Chip Nataro\*

Oxidation of  $[\text{Re}(\text{CO})_3(\text{dippf})\text{Br}]$  (dippf = 1,1'-bis(diiso-propylphosphino)ferrocene)  
yields  $[\text{Re}(\text{CO})_3(\text{dippf})\text{Br}]^+$ , the first structurally characterized complex of a coordinated  
bis(phosphino)ferrocenium ligand.

For table of contents use only